SYNTHESIS AND OPTICAL CHARACTERIZATION STUDIES OF RARE-EARTH DOPED TiO_2/PVDF HYBRID MEMBRANES

A minor research project report
Submitted to the

UNIVERSITY GRANTS COMMISSION

ज्ञान-विज्ञान विमुक्तये

BY

Prof. Rani George

Assistant Professor

1884-MRP/14-15/KLMG019/UGC-SWRO

Acknowledgment

I would like to thank God Almighty for his abundant blessings throughout my project work.

It is with pleasure that we express our sincere gratitude to Dr. N.V. Unnikrishnan for his valuable guidance and keen interest throughout the progress of the work which helped in clarifying the ideas.

I acknowledge with thanks the support in the form of financial assistance from university grants commission, ***New Delhi*** *for sanctioning the project.*

I express my sincere gratitude to all faculties of Dept.of physics, St.Aloysius College Edathua for their constant encouragement.

We are thankful to Mahatma Gandhi University for providing some of the experimental facilities.

Prof. Rani George

CHAPTER 1

General Introduction

Abstract

This chapter deals with the preparation of hybrid organic-inorganic nanocomposites and their applications.The properties of gadolinium and poly (vinylidene fluoride)(PVDF)/titanium dioxide nanoparticle are also discussed. Organic–inorganic hybrid materials do not represent only a creative alternative to design new materials and compounds for academic research, but their improved or unusual features allow the development of innovative industrial applications. Nowadays, most of the hybrid materials that have already entered the market are synthesised and processed by using conventional softchemistry based routes developed in the eighties.

1.1 Hybrid materials

Hybrid materialsare composites consisting of two constituents at the nanometeror molecularlevel. Commonly one of these compounds is inorganicand the other one organicin nature. Thus, they differ from traditional composites where the constituents are at themacroscopic (micrometerto millimeter) level. Mixing at the microscopic scale leads to a more homogeneous material that either shows characteristics in between the two original phases or even new properties.Many natural materials consist of inorganic and organic building blocks distributed on the nanoscale. In most cases the inorganic part provides mechanical strength and an overallstructure to the natural objects while the organic part delivers bonding between the inorganic building blocks and/or the soft tissue. Typical examples of such materials are bone, or nacre. The first hybrid materials were the paints made from inorganic and organic components that were used thousands of years ago. Rubber is an example of the use of inorganic materials as fillers for organic polymers.

The sol–gel process developed in the 1930s was one of the major driving forces what has become the broad field of inorganic–organic hybrid materials.Hybrid materials can be classified based on the possible interactions connecting the inorganic and organic species.*Class I* hybrid materials are those that show weak interactions between the two phases, such as van der Waals, hydrogen bonding or weak electrostaticinteractions. *Class II* hybrid materials are those that show strong chemical interactions between the components such as covalent bonds. Structural properties can also be used to distinguish between various hybrid materials.

1.1.1 Advantages of hybrid materials over traditional composites

Inorganic clusters or nanoparticles with specific optical, electronic or magnetic properties can be incorporated in organic polymer matrices.Contrary to pure solid state inorganic materials that often require a high temperature treatment for their processing, hybrid materials show a more polymer-like handling, either because of their large organic content or because of the formation of crosslinked inorganicnetworks from small molecular precursors just like in polymerization reactions.Light scattering in homogeneous hybrid

material can be avoided and therefore optical transparency of the resulting hybrid materials and nanocomposites can be achieved.

Two different approaches can be used for the formation of hybrid materials.Inbuilding block approach,building blocks at least partially keep their molecular integrity throughout the materialformation, which means that structural units that are present in these sources for materialsformation can also be found in the final material. The in situ formation of the hybrid materials is based on the chemical transformation of theprecursors used throughout materials' preparation.

1.1.2 Applications of hybrid organic–inorganic nanocomposites

The main applications of hybrid organic-inorganic nanocomposites is the decorative coatings obtained by the embedding of organic dyes in hybrid coatings and theScratch-resistant coatings with hydrophobic or anti-fogging properties.They are used for nanocomposite based devices for electronic and optoelectronic applications includinglight-emitting diodes, photodiodes, solar cells, gas sensors and field effect transistors and also in fire retardant materials for construction industry.Nanocomposite based dental filling materials is another application of this.The composite electrolyte materials for applications such as solid-state lithium batteries orsupercapacitors can be constructed. Other applications of organic-inorganic hybrid nanocomposites are proton conducting membranes used in fuel cells, antistatic / anti-reflection coatings and corrosion protection. Looking to the future, there is no doubt that these newgenerations of hybrid materials, born from the very fruitful activities in this research field, willopen a land of promising applications in many areas: optics, electronics, ionics, mechanics,energy, environment, biology, medicine for example as membranes and separation devices,functional smart coatings, fuel and solar cells, catalysts, sensors, etc.

1.2 Polyvinylidene fluoride (PVDF)

Polyvinylidenefluoride, or polyvinylidenedifluoride (PVDF) is a highly non-reactive thermoplastic fluoropolymer produced by the polymerization of vinylidenedifluoride. The Chemical formula of PVDF is $(C_2H_2F_2)_n$.PVDF is a specialty plastic used in applications

requiring the highest purity, as well as resistance to solvents, acids and bases. Compared to other fluoropolymers, likepolytetrafluoroethylene (Teflon), PVDF has a low density (1.78 g/cm3). It is available as piping products, sheet, tubing, films, plate and an insulator for premium wire. It can be injected, molded or welded and is commonly used in the chemical, semiconductor, medical and defense industries, as well as in lithium-ion batteries. It is also available as a crosslinked closed-cell foam, used increasingly in aviation and aerospace applications. Poly(vinylidene fluoride) (PVDF) is a frequently usedmaterial in the manufacturing of ultrafiltration (UF), microfiltration (MF), and pervaporation (PV) membranes due to its competent properties, such as excellent thermal and chemical stability, radiation resistance, etc. Many investigations have been done on the PVDF membranes. Some researchers focused on their application in water treatment, and the others concentrated on themembrane formation mechanism. However, the strongfouling propensity of PVDF membranes poses challenges,especially the significant nonspecific adsorption of organicsdue to the intrinsic low surface energy and hydrophobicityof PVDF polymer.

PVDF membranes are used for western blots for immobilization of proteins, due to its nonspecific affinity for amino acids. When poled, PVDF is a ferroelectric polymer, exhibiting efficient piezoelectric and pyroelectric properties. These characteristics make it useful in sensor and battery applications.

1.3 Titanium dioxide

Titanium dioxide, also known as titanium(IV) oxide or titania, is the naturally occurring oxide of titanium, (TiO_2). When used as a pigment, it is called titanium white.It has a wide range of applications, from paint to sunscreen to food colouring. One method for the production of titanium dioxide with relevance to nanotechnology issolvothermal synthesis of titanium dioxide Solvothermal synthesis is a method of producing chemical compounds. It is very similar to the hydrothermal route (where the synthesis is conducted in a stainless steel autoclave), the only difference being that the precursor solution is usually not aqueous (however, this is notalways the case in all literature uses of the expression).The molar mass of titanium dioxide is 79.866 g/mol. Among the inorganic nanoparticles, titanium dioxide (TiO_2) is quite popular for its innocuity, resisting and decomposing bacteria, UV- proof and super hydrophilicity. Many polymer/TiO2 nanocomposite membranes were prepared by simply incorporating TiO2nanoparticles into the polymer matrix , but there is still much to be done.

1.4 Gadolinium

Gadolinium is a chemical element with symbol Gdand atomic number 64. It is a silvery-white,malleable and ductile rare-earth metal. It is found in nature only in combined (salt) form. Gadolinium was first detected spectroscopically in 1880 by de Marignac who separated itsoxide and is credited with its discovery. It is named for gadolinite, one of the minerals in which it was found, in turn named for chemist Johan Gadolin and the metal was isolated by Paul. Gadolinium metal possesses unusual metallurgic properties, to the extent that as little as 1%gadolinium can significantly improve the workability and resistance to high temperatureoxidation of iron, chromium, and related alloys. Gadolinium as a metal or salt hasexceptionally high absorption of neutrons and therefore is used for shielding in neutronradiography and in nuclear reactors. Like most rare earths, gadolinium forms trivalent ionswhich have fluorescent properties.Gadolinium demonstrates a magnetocaloric effect whereby its temperatureincreases when it enters a magnetic field and decreases when it leaves the magnetic field.

Gadolinium combines with nitrogen, carbon, sulfur, phosphorus, boron, selenium, silicon and arsenic at elevated temperatures, forming binary compounds.Unlike other rare earth elements, metallic gadolinium is relatively stable in dry air. Gadolinium is a strong reducing agent, which reduces oxides of several metals into their elements. Gadolinium is quite electropositive and reacts slowly with cold water and quitequickly with hot water to form gadolinium hydroxide:

$2\ Gd + 6\ H_2O \longrightarrow 2\ Gd(OH)_3 + 3\ H_2$

Gadolinium is a constituent in many minerals such as monazite and bastnäsite, which are oxides. The metal is too reactive to exist naturally. Ironically, as noted above, the mineral gadolinite actually contains only traces of Gd. The abundance in the earth crust is about 6.2 mg/kg.

1.5 Samarium

Samarium is one of the rare earths in the lanthanide group, with atomic number 62. It was revealed spectroscopically by its sharp absorption lines in 1879 by Lecoq de Boisbaudran in the mineral samarskite. It is found along with other members of the rare earth elements in many minerals, including monazite and bastnasite. It has a bright silver luster and is reasonably stable in air. Its ionic radius is 1.08 Å. The electronic configuration is [Xe] $6s^2$ $4f^6$. The optical properties of Sm^{3+} ions are due to the transition between the partially filled 4f levels. The different transition levels for Sm^{3+} ion is shown in Figure 1.4. The ground state is $^6H_{5/2}$ and the luminescent transition originates from $^4G_{5/2}$, $^4F_{3/2}$ and $^4G_{7/2}$ levels.

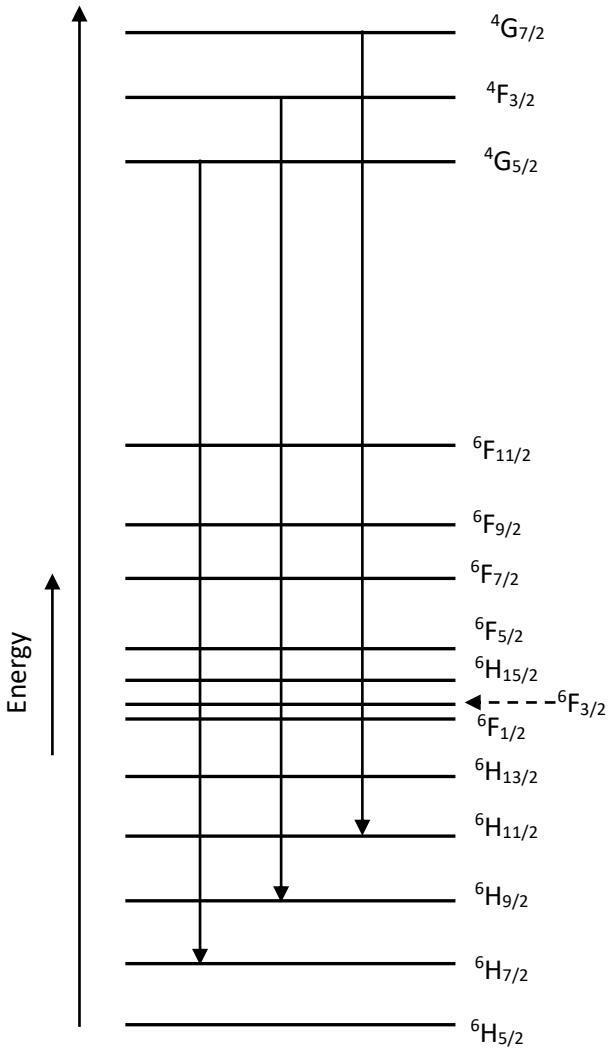

Transition levels of Sm^{3+} ions

References

1.Standard Atomic Weights 2013 . Commission on Isotopic Abundances and Atomic Weights

2. Du J R, Peldszus S, Huck P M, Feng X. Modification of poly(vinylidene fluoride) membranes

3. Cao X, Ma J, Shi X, RenZ.Applied Surface Science, 2006, 253(4): 2003–2010)

CHAPTER 2

Characterization Techniques

Abstract

This chapter deals with the Spectroscopic techniques, UV-Visible and photoluminescence spectroscopies and FTIR techniques which are used for the analysis of prepared sample.

Instrumentation techniques

Poly(vinylidene fluoride) (PVDF)/titanium dioxide (TiO_2) hybrid membranes were prepared using nano-TiO_2 as the modifier, and characterized by photoluminescence spectroscopy,UV-visible spectroscopy and fourier transform infrared spectroscopy (FTIR).This group of techniques use a range of principles to reveal the chemical composition,composition variation, crystal structure and photoelectric properties of materials.

2.1 UV-Visible Spectrometer

UV-Vis spectroscopy refers to absorption spectroscopy or reflectance spectroscopy in the ultraviolet visible spectral region. UV-vis spectroscopy is based on the principle of electronic transition in atoms or molecules upon absorbing suitable energy from an incident light that allows electrons to excite from a lower energy state to higher excited energy state. While interaction with infrared light causes molecules to undergo vibrational transitions, the shorter wavelength with higher energy radiations in the UV (200-400 nm) and visible (400-700 nm) range of the electromagnetic spectrum causes many atoms/molecules to undergo electronic transitions.

The fraction of sunlight that can be absorbed is specific for each material and varies with its chemical structure. Band gap and molecular energy levels control are of crucial importance for device performance. The mismatch of the polymer absorption spectra and the solar irradiance spectrum is one of the reasons for low efficiencies of devices. Chemical modification of the semiconducting polymers structure is a common approach that leads to tuning of the band gaps. The extension of conjugation degree leads to an enhancement, in terms of intensity, and red-shift of the absorption spectra of conjugated polymers. The energy levels also determinate the selection of electrodes and conducting materials. The alignment of the polymer on the film plays an important role in the solar cell device performance since it affects carrier mobility. Organic conducting polymers posses an anisotropic structure and the conductivity is higher along the chain direction, provided by π-π overlap between successive monomers, when the conjugated polymer films are macroscopically ordered. The maximum absorption wavelength, , of the polymer in the solid state is, in general, bathochromically shifted when compared to the solution spectra, due to majorconformational order, resulting indifferent energy levels distribution. Another way to improve the absorption by reorganizing the intermolecular packing, therefore changing the properties of the material, is through the

annealing process. The maximum absorption increases and broadens to a longer wavelength for corresponding transitions.This means that because the optical absorption corresponds to differences in energy states, it can be considered an indirectmeasure of the electronic structure. The optical band gap , expressed in electronvolts, depends on the incident photon wavelength by means of a Planck relation

$$E_{opt} = h\nu = \frac{hc}{\lambda} \qquad (2.1)$$

whereh is the Planck constant,ν is the wave frequency and c is the lightspeed in vacuum. Experimentally, the optical band gap of the polymer thin film is estimated by linear extrapolation from the absorption feature edge to and subsequent conversion of the wavelength (nm) into energy value versus vacuum (eV).

Since the absorption spectrum reveal information on electronic transition, the onset of absorption is considered as the bandgap of semiconductor or conjugated polymers. Many also consider the peak of the absorption spectrum as the band gap. Generally, the color of a molecule in solution or film gives an indication of their band gap. The color of a film or solution that an observer perceives is usually the complementary wavelength of the electromagnetic spectrum that the molecule absorbs.

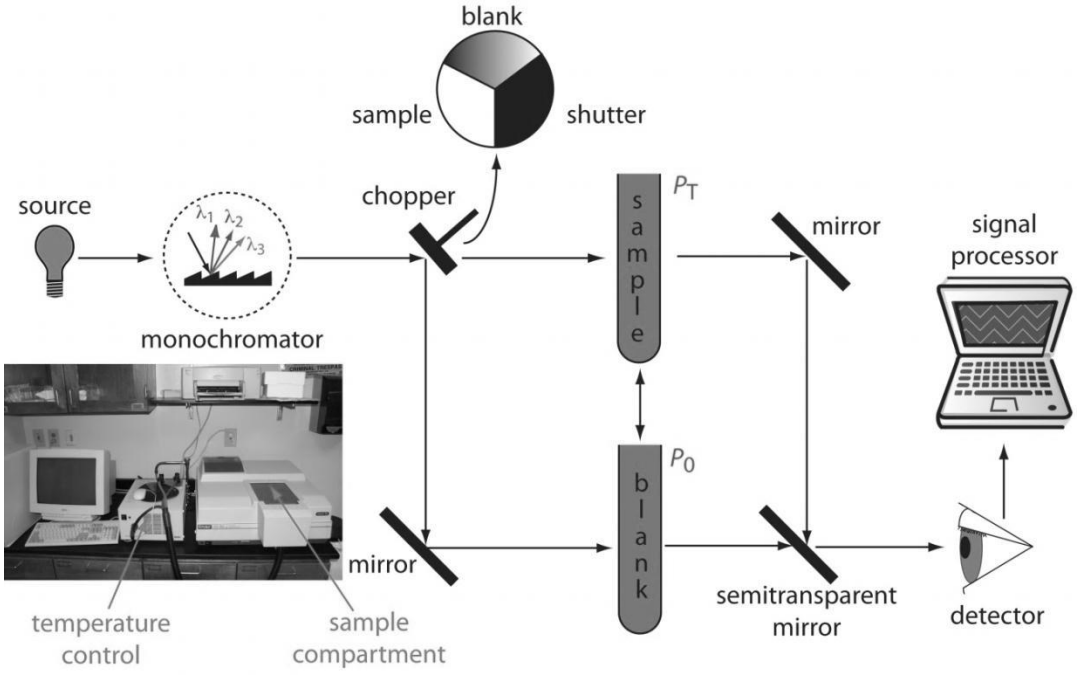

Figure 2.1 represents the schematic diagram of a UV-Vis spectrometer

2.2 Photoluminescence Spectroscopy

Photoluminescence (PL) spectroscopy is a contactless, nondestructive method to probe the electronic structure of materials. Our capabilities include: various excitation wavelengths that allow for varying levels of volume excitation; a detection range extending from 0.4 to 2.7 μm; sample temperatures of 4 to 300 K; and mapping capabilities with 1- to 2-μm spatial resolution on the Fourier-transform-based system. The intensity and spectral content of the emitted photoluminescence is a direct measure of various important materialproperties, including:

1.**Bandgap Determination:** The spectral distribution of PL from a semiconductor can be analyzed to nondestructively determine the electronic bandgap. This provides a means to quantify the elemental composition of compound semiconductor and is a vitally important material parameter influencing solar celldevice efficiency.

2.**Impurity Levels and Defect Detection:** The PL spectrum at low sample temperatures often reveals spectral peaks associated with impurities contained within the host material. The high sensitivity of this techniqueprovides the potential to identify extremely low concentrations of intentional and unintentional impurities that can strongly affect material quality and device performance.

3.**Recombination Mechanisms:** The quantity of PL emitted from a material is directly related to the relative amount of radiative and nonradiative recombination rates. Nonradiative rates are typically associated with impurities and thus, this technique can qualitatively monitor changes in material quality as a function of growth and processing conditions.

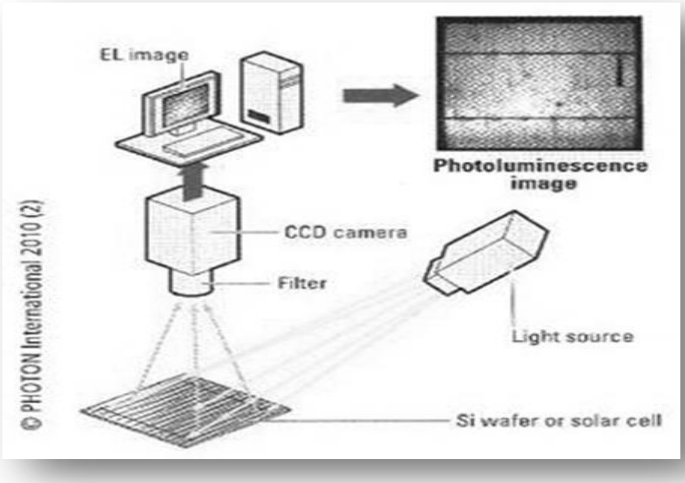

Figure 2.2 schematics of photoluminescence

2.3 FT-IR Spectroscopy

Fourier Transform Infra-Red spectroscopy (FT-IR) has wide applicability in structure elucidation, which are either synthesized chemically or of natural origin. Now a day, Fourier Transform Infra-Red (FT-IR) Spectroscopy is extensively used for quantitative as well as for qualitative analysis in almost all fields of science. It has many advantages and applications as compared to dispersive infra red technology.

FT-IR stands for Fourier Transform Infra Red, the preferred method of infrared spectroscopy. In infrared spectroscopy, IR radiation is passed through a sample. Some of the infrared radiation is absorbed by the sample and some of it is passed through (transmitted). The resulting spectrum represents the molecular absorption and transmission, creating a molecular fingerprint of the sample.

- It can identify unknown materials
- It can determine the quality or consistency of a sample
- It can determine the amount of components in a mixture

An infrared spectrum represents fingerprint of a sample with absorption peaks which correspond to the frequencies of vibrations between the bonds of the atoms making up the material. Because each different material is a unique combination of atoms, no two compounds produce the exact same infrared spectrum. Therefore, infrared spectroscopy can result in a positive **identification** (qualitative analysis) of every different kind of material. In addition, the size of the peaks in the spectrum is a direct indication of the **amount** of material present. With modern software algorithms, infrared is an excellent tool for quantitative analysis.

Experimental arrangement of FT-IR is shown in fig.2.3. The normal instrumental process is as follows:

1. The Source: Infrared energy is emitted from a glowing black-body source. This beam passes through an aperture which controls the amount of energy presented to the sample (and, ultimately, to the detector).

2. The Interferometer: The beam enters the interferometer where the "spectral encoding" takes place. The resulting interferogram signal then exits the interferometer.

3. The Sample: The beam enters the sample compartment where it is transmitted through or reflected off of the surface of the sample, depending on the type of analysis being accomplished. This is where specific frequencies of energy, which are uniquely characteristic of the sample, are absorbed.

4. The Detector: The beam finally passes to the detector for final measurement. The detectors used are specially designed to measure the special interferogram signal.

5. The Computer: The measured signal is digitized and sent to the computer where the Fourier transformation takes place. The final infrared spectrum is then presented to the user for interpretation and any further manipulation.

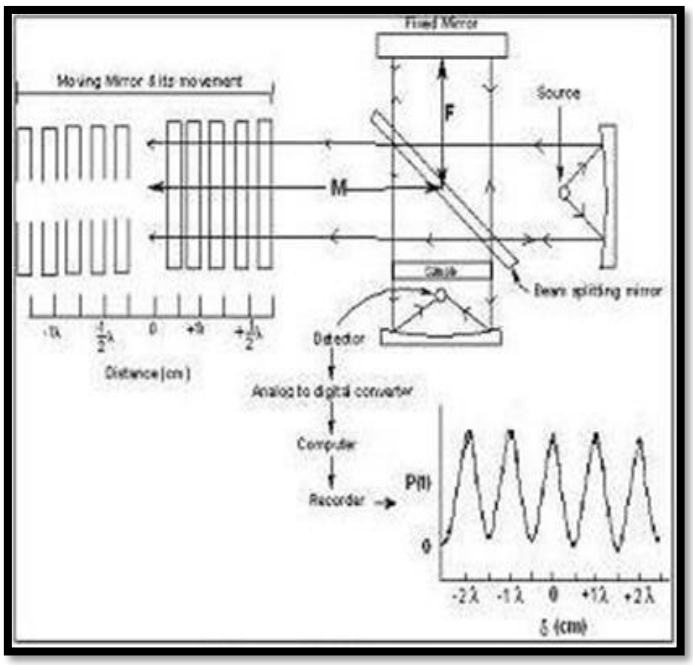

Figure 2.3 FT-IR Instrumentation

FT-IR consists of a moving mirror, fixed mirror, beam splitter, IR radiation source and detector. Instead of using monochromator, Michelson interferometer is used for analysis of IR radiation after passing through sample.Radiation from IR source is collimated by mirror and the resultant beam is divided at beam splitter. Half of beam

passes through mirror (fixed) and half refracted to moving mirror. After reflection by these two mirrors, two beams recombined at beam splitter and passes through cell and after that radiation is focused to detector. Movable mirror, moves back and forth at a distance of 21 cm. If round trip distance between beam splitter and fixed mirror is identical to that of beam splitter and movable mirror, then only the radiation from two mirrors arise in phase at beam splitter, cell and to detector. As the movable mirror changes its position, the distance between mirror and beam splitter no longer identical and radiation of fixed wavelength will arrive in phase only to cell and detector. So we have to add or subtracts whole number of multiple of wavelength of radiation in round trip distance between splitter and fixed mirror. If movable mirror moves by a factor $\lambda/4$, then round trip distance is altered by $\lambda/2$ reflected radiation if **out of phase** with that from stationary mirror and interferes destructively while movable mirror moves by a factor $\lambda/2$, then round trip distance is altered by $\lambda/2$ reflected radiation if **in phase** with that from stationary mirror and interferes **constructively**.

The radiation striking the detector, after passing through MI will be of lower frequency than source frequency. One cycle of the signal occurs when the mirror moves at a distance that corresponds to half of wavelength ($\lambda/2$,). If the mirror is movingat constant velocity and we define τ as the time required for mirror to move distance of $\lambda/2$. As the distance changes, wavelength of radiation beams becomes in phase or out of phase depending on wavelength of incident radiation and rate at which movable mirror moves. So that by controlling the rate of mirror motion a series of simultaneous signals that oscillate frequency which is directly proportional to EMR frequency arrive at detector and oscillate slowly for detector to measure. The detector simultaneously measures all of frequencies that pass through the cell and routes the information to computer and this information are decoded by FT and decoded spectrum is directed to read out device. Time from insertion of sample to recording of plot is about 2 min.

References

[1]. E.Snitzer, Phys. Rev. Lett. 7(1961)444

CHAPTER 3

Optical Characterization of Gd^{3+} doped PVDF/TiO_2 hybrid material

Abstract

This chapter deals with the experimental procedures which are used for the preparation of desired samples. It also contains studies based on the absorption and excitation – emission spectral data.

3.1 Introduction

The sol-gel process, which is mainly based on inorganicpolymerization reactions, is a chemical synthesis method initially used for the preparation of inorganic materials such as glasses and ceramics. Its unique low temperature processing characteristic also provides unique opportunities to make pure and well-controlled composition organic/inorganic hybrid materials through the incorporation of low molecular weight and oligomeric/ polymeric organic molecules with appropriate inorganic moieties at temperatures under which the organics can survive. The organic/inorganic hybrid materials made in this way, which have been termed “ceramers” by Wilkes et al.1 and “ormosils” or “ormocers” by Schmidt et al.,2are normally nanocomposites and have the potential for providing unique combinations of properties which cannot be achieved by other materials. For the past decade, organic/inorganic nanocompositesprepared by the sol-gel process have attracted a great deal of attention, especially in the fields of ceramics, polymer chemistry, organic and inorganic chemistry, and physics. The preparation, characterization, and applications of organic/inorganic hybrid materials have become a fast expanding area of research in materials science. The major driving forces behind the intense activities in this area are the new and different properties of the nanocomposites which the traditional macroscale composites and conventional materials do not have.

3.2 Synthesis

PVDF –TiO_2doped with Gd^{3+}were prepared through sol- gel route with PVDF and titanium isopropoxide(TIP) as precursors in the presence of ethanol. The dopant, Gadolinium is added in the form of oxide. The DMF(dimethyl formamide,$(CH_3)_2NCH$),which is the common solvent for chemical reactions, was used as the solvent for PVDF.One gram of PVDF/TiO_2 sample were prepared with composition of 50:50 and dopant concentration was maintained at 5%. The resulting mixture was stirred continuously using a magnetic stirrer for about half an hour at room temperature till it formed a clear solution. A glass substrate is cleaned and the mixture was dip coated into the silica glass substrate. The film was uniform. The remaining mixture (sol) is poured into poly propylene containers, which is sealed and kept to form stiff gel for month. The samples were clear, transparent. The Gd^{3+} doped sample was heated at 250℃ for one hour. The excitation & emission spectra were taken using photoluminescence spectrometer, the absorption spectra

were measured with UV-Vis spectrophotometer (Shimadzu- UVPC 2401) and FTIR spectra were taken for structural elucidation.

3.2 Results and Discussion

3.2.1 Absorption Studies

The direct absorption band gap of the sample can be determined by fitting the absorption data to the Tauc equation

$$Ah\nu = B\,(h\nu - E_g)^{1/2} \qquad \ldots\ldots(3.1)$$

In which $h\nu$ is the photon energy, α is the absorption co efficient,$E_g$is the absorption band gap and B is a constant relative to the material. The absorption coefficient can be obtained from the equation

$$\alpha = \frac{(2.303\,A)}{d} \qquad \ldots\ldots(3.2)$$

Where A is the absorbance and d is the thickness of the sample. The plot of $\sqrt[2]{\alpha h\nu}$ versus $h\nu$ is shown in the Figure 3.2.The variation of intensity of absorption with wavelength is shown as inset. It gives the value of band gap as 5.25eV

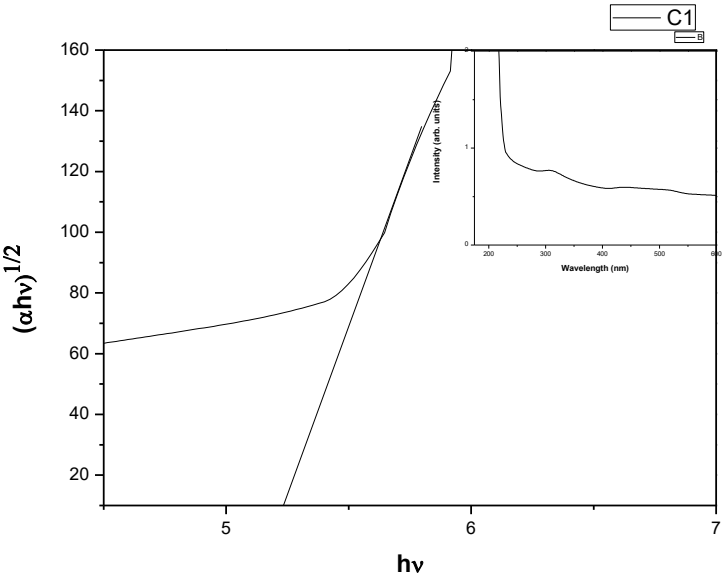

Figure3.2 Plot of $\sqrt[2]{\alpha h\nu}$ versus $h\nu$ for the determination ofoptical band gap of PVDF/TiO_2 doped Gd^{3+} hybrid material.

3.3.2 Emission and excitation studies

Figure 3.5 shows the fluorescence spectra of PVDF/TiO_2 doped Gd^{3+}.

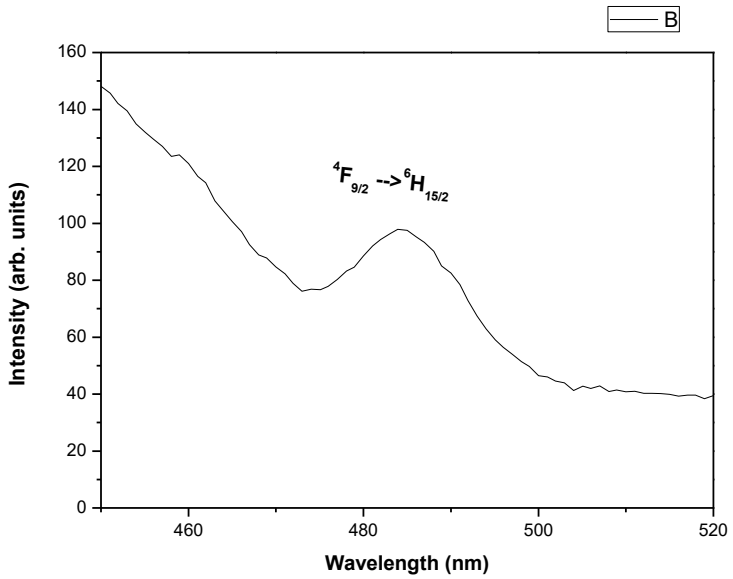

Figure 3.3 Emission spectra of PVDF/TiO_2 doped Gd^{3+} hybrid material.

The emission peak at 482nm corresponding to the transition $4F_{9/2} \rightarrow 6H_{11/2}$ is the most intense one.

Figure3.7 shows the excitation spectrum taken with an emission wave length of 550 nm. This shows different transitions associated with the PVDF/TiO_2 doped Gd^{3+} sample.The absorption peaks are at 345nm and 408nm corresponding to the transitions $8H_{16/2} \rightarrow 8P_{7/2}$ and $6H_{15/2} \rightarrow 4I_{13/2.}$

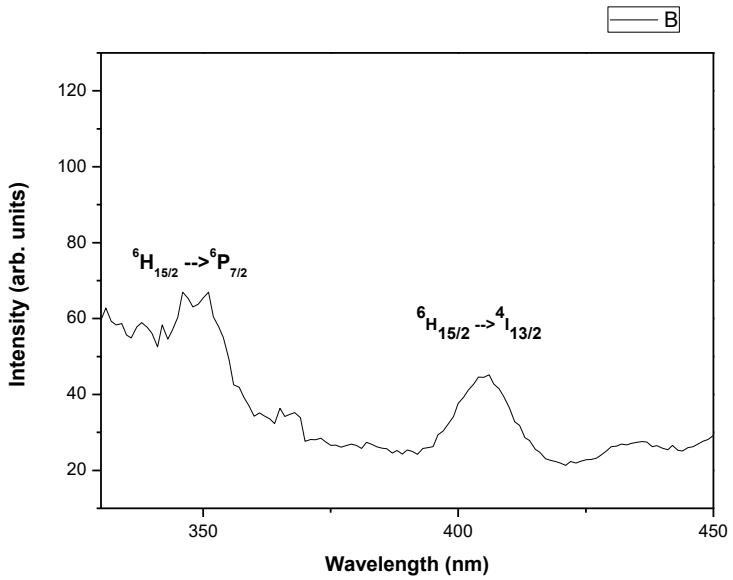

Figure 3.4 shows the excitation spectra of PVDF/ doped Gd^{3+} hybrid material.

3.3.3 FTIR studies

FTIR spectrum of finely powdered sample is taken.Usually, the PVDF is in a semi crystalline phases (α and β) and an amorphous phase. Peak at 1179 cm^{-1} wereattributed to the phase vibration of β crystalline. The peak at 1403 cm^{-1} was due to the deformation vibration of $–CF_2$.Compared with pure PVDF membranes, a new absorptionband around 609 cm^{-1} could be found in the FT-IR spectraof PVDF/TiO_2, which could be ascribed to the symmetric deformation vibration of Ti–O–Ti group. It indicated that the TiO_2 were embedded and dispersed within the hybrid membranes. Besides, the absorption peaks appearing at the interval of 3300–3400 cm^{-1} were assigned to the stretching vibration of –OH groups, which also indicated the presence of TiO_2 in the hybrid material.

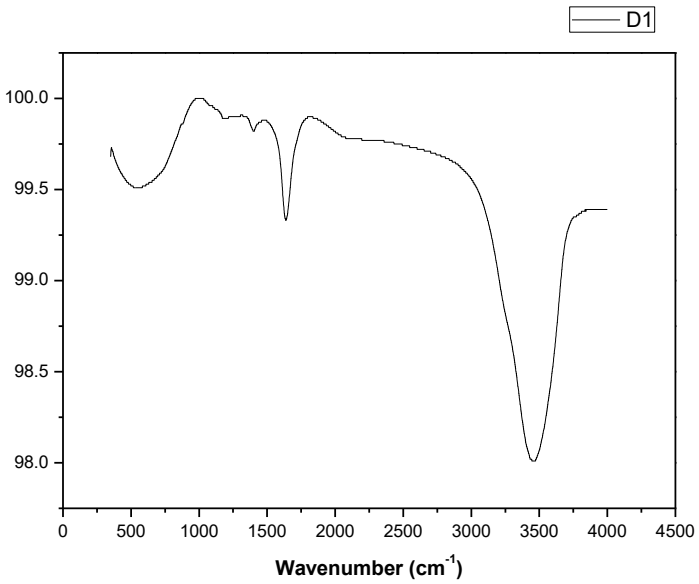

Fig.3.5: FTIRspectra of PVDF/TiO_2 doped Gd^{3+} hybrid material

The absorption peaks at around1600 cm–1 could be assigned to the vibration of the Ti–O bond, the intensity of which became stronger with the

increase in TiO_2 content. It could also be observed thatwith the addition of nano-TiO_2, a peak appears due to thevibration of the PVDF β phase, which further proved thatthe stress was the main reason for the change in PVDF crystal formation. Therefore, the FT-IR spectra clearlydemonstrated that TiO_2 was successfully incorporated intothe PVDF material.

References

[1]. Journal of Physics and Chemistry of solidsFluorescence characteristics of PVDF/TiO_2 nanocrystals doped gadolinium P.V.Jyothy, K.A. Amrutha, Joseph Xavier, N. V. Unnikrishnan

[2]. S.TamilSelvan,T.Hayakawa,M.Nogami,J.Non-cryst.solids 29(2001)1137.

[3]. E.J.C.Dawny, M.A.Fardad,M.Green,E.M.Yeatman,J.Mater. Res.12 (1997)3115.

[4]. L.E.Brus, J.Chem.Phys.79 (1983)5566.

[5]. Y.Kayanuma, Phys.Rev.B 389(1998)797

[6]. S.TamilSelvan,T.Hayakawa,M.Nogami,J.Sol-Gel Sci.Tech.19(2000) 779.

[7]. K.Annapurna, R.Dwivedi, P. Kundu, S.Buddhudu, Mater.Res.Bull.38 (2003) 429.

[8]. J.Maab, M.Wollenhaupt, H. Ahrens, P. Frobel, K.Barner, J.Lumim 62 (1994) 95.

[9]. H.Okamoto, J.Matsuoka, H.Nasu, K.Kamiya, H.Tanaka, J.Appl.Phys.75 (1994) 2251

[10]. J.Malhotra,D.J.Hagan,B.G.Potter,J.OptSoc.Am.B 8(1991) 1531.

[11]. S.TamilSelvan, T.H.M.Nogami, J.Non-Cryft.Solids141 (2001)291137.

[12]. G.G.Yordanov, E.Adachi,C.D.Dushkin,ColloidsSurf.A289(2006)118.

[13]. C.de Mello Donega, M.Bode, A.Meijerink, Phys.Rev.B74 (2006)085320.

CHAPTER 4

Optical Characterisation of Samarium doped PVDF/TiO_2 hybrid material

Abstract

This chapter deals with the experimental procedures which are used for the preparation of samarium doped PVDF/TiO_2 hybrid samples. It also contains studies based on the absorption and excitation – emission spectral data. Also the bandgap and bonding parameter is determined for one sample.

4.1 Introduction

Polymer nanocomposites combine peculiar characteristics of polymers, such as structural flexibility, convenient processability and high thermal and mechanical stability with specific size dependent properties of inorganic nanocrystalline oxides, thus providing unique functions. Such cooperative combination helps to fabricate unique materials with properties favourable in many application fields including light-emitting diodes, optical switches, waveguides, transparent coatings and sensors [1–7].

In the past few decades, organic–inorganic hybrid composites had gained considerable attention in many applications. One of the main reasons is the wide variety of controllable optical, mechanical and electrical properties that can be tuned by tailoring the organic and inorganic moieties into nanosized domains. New optoelectronic materials based on these nanocomposites have been widely reported, such as those for optical coatings, optical switches, contact lenses, high refractive index devices, optical waveguides and nonlinear optical devices [8-13]. Limitations of polymers for much higher performance applications can be improved by adding inorganic materials. Inorganic materials exhibit excellent thermal stability and functional properties such as dielectric and magnetic properties, but have high brittleness and bad film forming characteristics. Sol-gel synthesis of organic-inorganic hybrid materials for planar waveguides and devices has received growing interest due to its low cost processing and good suitability for doping and this synthesis technique also enables control of the organic–inorganic interaction at various molecular, nanometer and micrometer scales [14-16].

Titania/polymer nanocomposites represent a new class of potential materials for optoelectronic applications. Titanium dioxide (TiO_2) is a very promising material for applications in many aspects such as solar energy conversion, photocatalysis, sensors and photochromic devices [17, 18]. TiO_2 has three crystallographic phases: anatase, brookite and rutile [19]. Among them, anatase has been proved to have excellent photoactivity and optoelectronic properties [20, 21]. Non hydrolytic sol-gel techniques have been extensively used by researchers for the synthesis of transition-metal oxide nanocrystals [22, 23].

Generally, the inorganic/organic hybrid composite has potential applications in optical and cosmetic fields and food packing material. However, pure inorganic film has loose film

stress and poor compatibility with the substrate. PVDF with good film forming properties and mechanical properties may become additive of optical film to improve the film stress and compatibility with the substrate. Poly(vinylidene fluoride) (PVDF), as an industrially important semi-crystalline polymer, has found ever increasing applications in electronics with its outstanding electric and mechanical properties and ultrafiltration membrane with its excellent chemical resistance. PVDF has a complex crystalline polymorphism with four known polymorphs called a, b, c, and d. The a-polymorph is regarded as the most thermodynamically stable structure of PVDF and the rest three can be obtained at different solution-casting conditions and polymer blends. And b-phase PVDF, commonly used for pyro- and piezoelectric applications, is generally obtained by drawing the a-phase PVDF films at temperature range 70–87ºC [10, 11].

4.2 Synthesis

PVDF –TiO_2 doped with Sm^{3+} were prepared through sol- gel route with PVDF and titanium isopropoxide(TIP) as precursors in the presence of ethanol. The dopant, Samarium is added in the form of nitrate. The DMF (dimethyl formamide, $(CH_3)_2NCH$), which is the common solvent for chemical reactions, was used as the solvent for PVDF. One gram of PVDF/TiO_2 sample were prepared with different composition of PVDF and TiO_2 and dopant concentration was maintained at 5%. Following PVDF/TiO_2 hybrid materials namely

1. PT5050
2. PT2080Sm5
3. PT4060Sm5
4. PT5050Sm5
5. PT6040Sm5
6. PT8020Sm5

were prepared. The resulting mixture was stirred continuously using a magnetic stirrer for about half an hour at room temperature till it formed a clear solution. A glass substrate is cleaned and the mixture was dip coated into the silica glass substrate. The film was uniform. The remaining mixture (sol) is poured into poly propylene containers, which is sealed and kept to form stiff gel for month. The samples were clear, transparent. The Sm^{3+} doped sample was heated at $50℃$ for one hour. The excitation & emission spectra were taken using photoluminescence spectrometer and the absorption spectra were measured with UV-Vis spectrophotometer (Shimadzu- UVPC 2401).

4.3 Results and Discussion

4.3.1 Absorption Studies

Figures 1(a) and 1(b) show the absorption spectra of PT5050Sm5 hybrid material in the UV-Vis and NIR regions, respectively. The absorption spectra contain 18 bands corresponding to transitions of Sm^{3+} ions from the ground state $^6H_{5/2}$ to the various excited states. The distribution of crystal field in the matrix contributes to the inhomogeneous broadening of peaks in the spectra. The absorption band positions and its energy level assignments are reported in Table 2 [24]. From the absorption spectra, it is found that the NIR region contains most intense peaks. The NIR region contains several intense transitions from the ground state $^6H_{5/2}$ to the various ^6F terms of Sm^{3+} ions are spin-allowed transitions ($\Delta S = 0$). The transition from $^6H_{5/2}$ to the level $^6F_{1/2}$ is hypersensitive in nature for Sm^{3+} ions ($|\Delta J| \leq 2$, $\Delta S = 0$ and $\Delta L \leq 2$) and any local structural change may sharply effect the position and intensity of this transition.

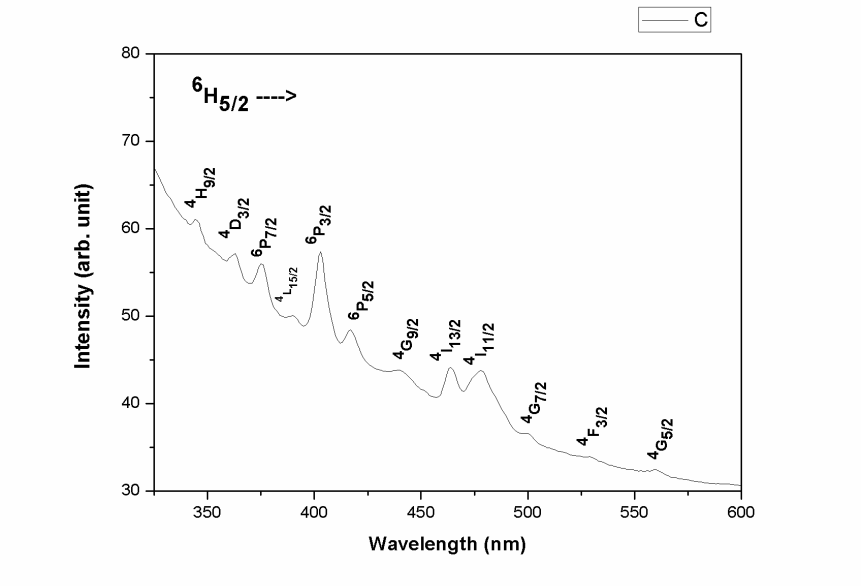

Fig 4.1(a) : UV Vis Absorption spectrum of PT5050Sm5

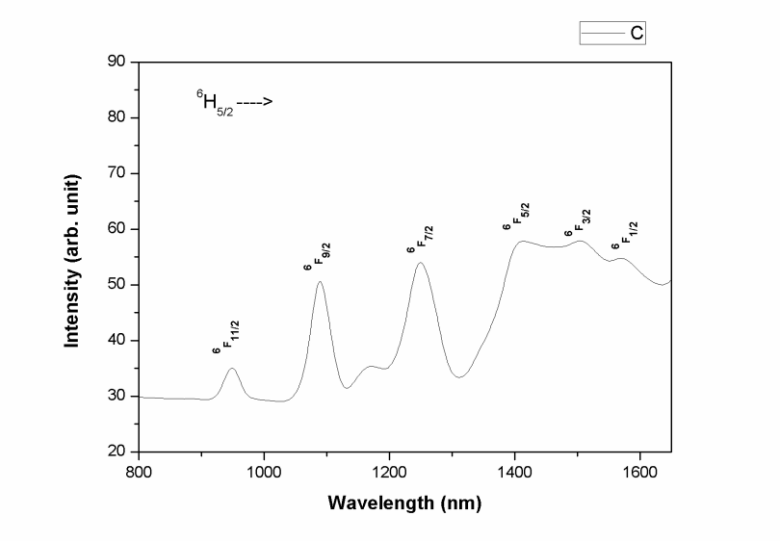

Fig 4.1(b) : NIR Absorption spectrum of PT5050Sm5

The absorption studies of different concentrations of the prepared sample at the excitation wavelength of 400 nm are shown in figure 4.4. The transitions are similar as that for PVDT5050Sm5.

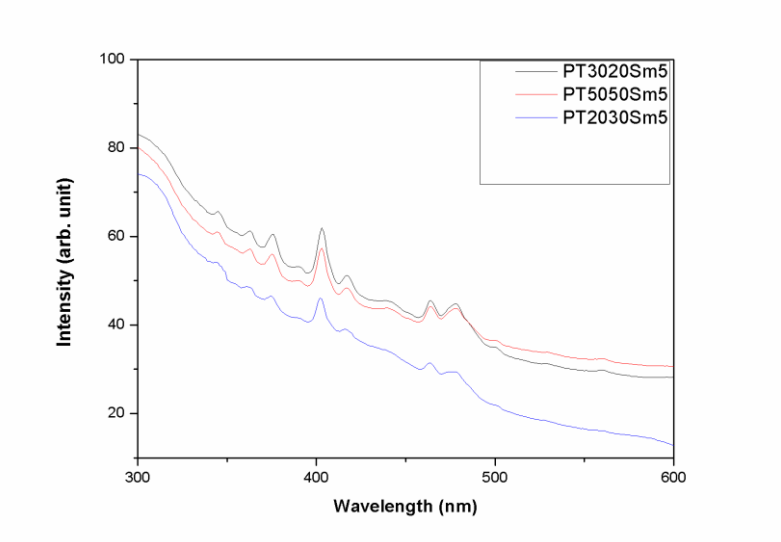

Figure 4.1 (c) Absorption spectra of PVDF/TiO_2 doped Sm^{3+} hybrid material for different concentrations of PVDF and TiO_2.

4.3.1.1 Energy Band gap (E_g)

The optical absorption coefficient, $\alpha(\nu)$ for of PT5050Sm5 hybrid material was calculated using the following equation

$$\alpha(\nu) = \frac{A}{d} \quad (4.1)$$

where$A$ is the absorbance and d is the optical path length. The quantity, $\alpha(\nu)$ can be expressed by the relation

$$\alpha(\nu) = \frac{B(h\nu - E_g)^n}{h\nu} \quad (4.2)$$

whereE_g is the optical band gap energy and B is a constant [30]. The index,n can have any values between 0.5 and 3 depending upon the inter-band electronic transitions. The measured absorption fits well to the Eqn. (2) for direct allowed transitions, n = 0.5. Figure 2 shows the variation of α^2 versus photon energy for PT5050Sm5 hybrid material. It is noted that the optical energy band gap (E_g) for PT5050Sm5 hybrid material is 4.59 eV.

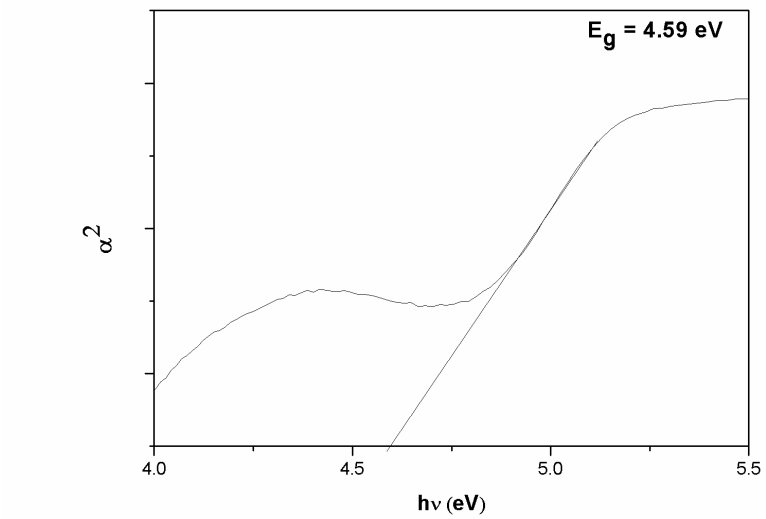

Fig 4.2 : Variation of α^2 versus $h\nu$ in PT5050Sm5

4.3.1.2 Nephelauxetic ratio and bonding parameter

The nature of the Sm^{3+}- ligand bond in the matrix can be inspected using Nephelauxetic ratio and bonding parameter. The nephelauxetic ratio (β) can be calculated by [25]

$$\beta = \frac{\nu_c}{\nu_a} \quad (4.3)$$

where ν_c is the energy (in cm^{-1}) for a particular transition in the host and ν_a is the energy (in cm^{-1}) of the same transition in aqueous solution [24]. The bonding parameter (δ) can be evaluated using the equation

$$\delta = \frac{1-\beta'}{\beta'} \times 100 \qquad (4.4)$$

where β' is the average value of nephelauxetic ratios for all the observed transitions in the absorption spectra. The Sm^{3+}- ligand bond may be covalent or ionic depending upon the positive or negative sign of the bonding parameter. The nephelauxetic ratios (β) and bonding parameter(δ) of the sample are presented in Table 4.1 and it is found that the nature of the Sm^{3+}- ligand bond in the present matrix is covalent.

Table 4.1 : Energies for Sm^{3+} : PT5050Sm5 sample (ν_c) and aquo-ion (ν_a) along with nephelauxetic ratio(β) and bonding parameter (δ)

Sl. No.	$S'J'L'$ $^6H_{15/2}$ →	ϑ_c (cm^{-1})	ϑ_a (cm^{-1})	β
1.	$^4H_{9/2}$	29069.77	29012	0.998961
2.	$^4D_{3/2}$	27548.21	27714	0.994520
3.	$^6P_{7/2}$	26666.67	26660	0.996885
4.	$^4L_{15/2}$	25641.03	25638	0.962140
5.	$^6P_{3/2}$	24813.9	24999	0.994545
6.	$^6P_{5/2}$	23980.82	24101	0.997123
7.	$^4G_{9/2}$	22779.04	22706	1.003482
8.	$^4I_{13/2}$	21551.72	21650	0.997765
9.	$^4I_{11/2}$	20920.50	21096	0.991493
10.	$^4G_{7/2}$	20080.32	20014	1.001712
11.	$^4F_{3/2}$	18903.59	18832	1.003802
12.	$^4G_{5/2}$	17889.09	17924	0.998052
13.	$^6F_{11/2}$	10570.82	10517	0.995040
14.	$^6F_{9/2}$	9174.312	9136	0.994713
15.	$^6F_{7/2}$	8012.821	7977	0.994729
16.	$^6F_{5/2}$	7072.136	7131	0.994550
17.	$^6F_{3/2}$	6648.936	6641	0.997251
18.	$^6F_{1/2}$	6369.427	6397	0.997476

$\beta' = 0.995235$

$\delta = 0.1004$ (covalent bonding)

4.4 Excitation spectra

Excitation spectrum of PT5050Sm5 hybrid material at the emission wavelength 597 nm is depicted in figure 3. The excitation spectrum consists of 2 peaks corresponding to the transitions from the ground state $^6H_{5/2}$ to the various excited states $^4D_{3/2}$ and $^6P_{3/2}$ at the wavelengths of 358 and 401 nm, respectively. The optical absorption spectrum of the sample in the UV-Vis region (figure 4.1(a)) is compared with this excitation spectrum and it is confirmed that these transitions of Sm^{3+} ions are similar.

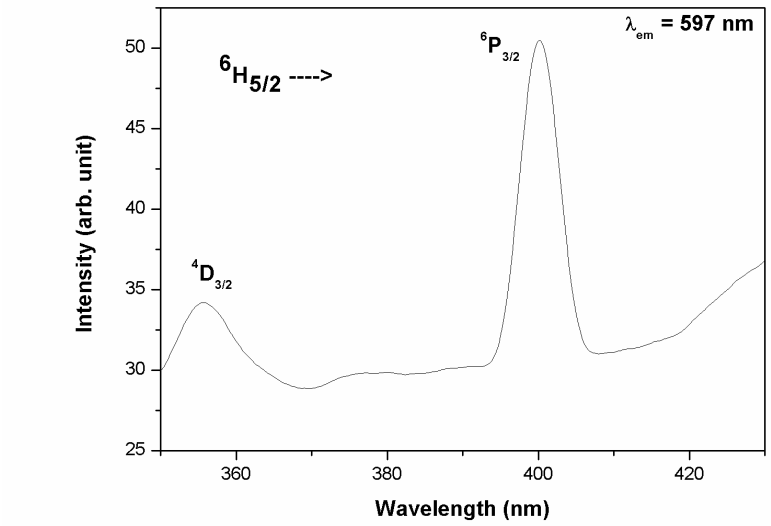

Fig 4.2 : Excitation spectrum of PT5050Sm5

4.5 Judd-Ofelt analysis

The experimental oscillator strength, (f_{exp}) of an absorption transition from the ground state to an excited state is expressed as

$$f_{exp} = 4.32 \times 10^{-9} \int \varepsilon(\nu) d\nu \qquad (4.5)$$

where$\varepsilon(\nu)$ is the molar absorptivity of a band at a wavenumber ν (cm^{-1}) and $d\nu$ is the half-band width [14]. According to Judd-Ofelt (JO) theory, the calculated oscillator strength of an absorption transition from the ground state ΨJ to an excited state $\Psi' J'$ is determined as

$$f_{cal} = \frac{8\pi^2 mc\nu}{3h(2J+1)} \frac{(n^2+2)^2}{9n} \sum_{\lambda=2,4,6} \Omega_\lambda \mid < \Psi J \parallel U^{(\lambda)} \parallel \Psi' J' > \mid^2 \quad (4.6)$$

Where Ω_λ is the JO intensity parameter, $\parallel U^{(\lambda)} \parallel^2$ is the doubly reduced matrix elements of unit tensor operator evaluated in the intermediate coupling approximation for the absorption transition and m denotes the mass of the electron [26,27]. A least-square fitting method is adopted for Eq. (2) to gauge Ω_λ parameters which give the best fit between experimental and calculated oscillator strengths. The quantity of the fit has been expressed by the root mean square (r.m.s.) deviation of oscillator strengths (σ).

$$\sigma = \left[\frac{\sum (f_{exp} - f_{cal})^2}{N_i}\right]^{1/2} \quad (4.7)$$

Where N_i denotes the total number of excited energy levels used for least-square fit.Spectroscopic quality factor of the glass can be expressed as

$$Q = \frac{\Omega_4}{\Omega_6} \quad (4.8)$$

Where Ω_4 and Ω_6 are long range parameters associated with the bulk properties of the matrix like viscosity and basicity. It is clear that Ω_λ values of PT5050Sm5 shown in Table 4.2 follow the trend as $\Omega_2 > \Omega_6 > \Omega_4$.The high value of Ω_2 parameter confirms the covalence of Sm^{3+}-O bond and low symmetry around Sm^{3+} ions, which is agreeable with the nephelauxetic effect (Table 4.1).

Table 4.2: Oscillator strength and JO parameter

Sl No	S, L' J' $^6H_{15/2}$ →	E_{exp} (cm^{-1})	E_{cal} (cm^{-1})	ΔE (cm^{-1})	Matrix elements			f_{exp} ($x10^{-6}$)	f_{cal} ($x10^{-6}$)	Δf ($x10^{-6}$)
					U(2)	U(4)	U(6)			
1	$^4H_{9/2}$	28972	29012	40	0.0001	0.0006	0.0006	0.0800	0.0111	0.0689
2	$^4D_{3/2}$	27529	27714	185	0.0001	0.0251	0.0000	0.0825	0.0807	0.0018
3	$^6P_{7/2}$	26634	26660	26	0.0000	0.0016	0.0751	0.1950	0.2331	-0.0381
4	$^4L_{15/2}$	25641	25638	3	0.0000	0.0000	0.0060	0.0227	0.0176	0.0052
5	$^6P_{3/2}$	24876	24999	123	0.0000	0.1680	0.0000	0.4424	0.4470	-0.0046
6	$^6P_{5/2}$	23981	24101	120	0.0000	0.0263	0.0000	0.0929	0.0673	0.0256

7	$^4G_{9/2}$	22779	22706	73	0.0001	0.0010	0.0028	0.0575	0.0154	0.0421
8	$^4I_{13/2}$	21598	21650	52	0.0000	0.0030	0.0228	0.0772	0.0631	0.0140
9	$^4I_{11/2}$	20921	21096	175	0.0000	0.0000	0.0108	0.1950	0.0258	0.1692
10	$^4G_{7/2}$	20040	20014	26	0.0004	0.0018	0.0025	0.0086	0.0297	-0.0211
11	$^4F_{3/2}$	18904	18832	72	0.0003	0.0000	0.0000	0.0091	0.0142	-0.0051
12	$^4G_{5/2}$	17889	17924	35	0.0002	0.0007	0.0000	0.0167	0.0103	0.0064

Ω_2= 1035.4×10^{-22} cm^2

Ω_4= 44.099×10^{-22} cm^2

Ω_6= 47.172×10^{-22} cm^2

σ = 0.056×10^{-6}

Q = 0.9349

4.3.2 Emission studies

Figure 3.5 shows the fluorescence spectra of Sm^{3+}doped PVDF/TiO_2 at the excitation wavelength 402 nm. The emission peaks occur at the wavelengths 565, 601, and 648 nm corresponding to the transitions from the emitting level $^4G_{5/2}$ to the levels $^6H_{5/2}$, $^6H_{7/2}$ and $^6H_{9/2}$ respectively. More intense transitions obtained at the wavelength 601 nm.

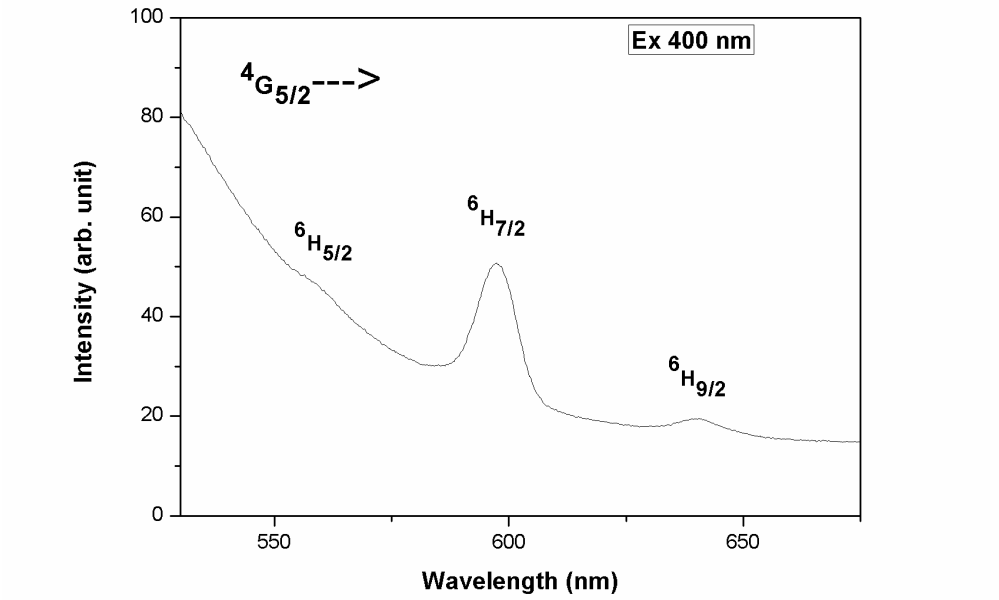

Figure 4.3 *Emission spectra of PVDF/TiO_2 doped Sm^{3+} hybrid material.*

4.5 CIE- COLOR COORDINATES

Appropriate combinations of blue and yellow emissions produce white light in addition to the generation and control of different colors in solid state display devices [57-60]. The white light that could be obtained by the emission of Dy^{3+}: LTT10 glass has been analyzed in the frame of the chromaticity color coordinates. The chromaticity coordinates *x* and *y* are calculated from the tri-stimulus values according to equations

$$x = \frac{X}{X + Y + Z} \tag{1.23}$$

$$y = \frac{Y}{X + Y + Z} \tag{1.24}$$

where *X*,*Y* and *Z* are the colour matching functions which give the stimulation for each of the three primary red, green and blue colours needed to match the degree of stimulation required to match the colour of $P(\lambda)$. The colour matching functions can be evaluated using the following equations [61]

$$X = \int_{\lambda} \bar{x}(\lambda) P(\lambda) d\lambda \tag{1.25}$$

$$Y = \int_{\lambda} \bar{y}(\lambda) P(\lambda) d\lambda \tag{1.26}$$

$$Z = \int_{\lambda} \bar{z}(\lambda) P(\lambda) d\lambda \tag{1.27}$$

The envelop of all monochromatic color coordinates makes the perimeter of Commission Internationale de I'Eclairage (CIE) 1931 chromaticity diagram . All the multichromatic wavelengths will lie within the area of chromaticity diagram. The color purity or color saturation of particular dominant color of a source is obtained by the distance in the chromaticity diagram between the emission color coordinates and the coordinates of equal energy point, divided by the distance between the equal energy point and the dominant wavelength point. Thus the color purity is given by

$$\text{Color purity} = \frac{\sqrt{(x - x_{ee})^2 + (y - y_{ee})^2}}{\sqrt{(x_d - x_{ee})^2 + (y_d - y_{ee})^2}} \tag{1.28}$$

where $(x, y), (x_{ee}, y_{ee})$ and (x_d, y_d) are the chromaticity coordinates of the emission light, equal energy point and the dominant wavelength points respectively.

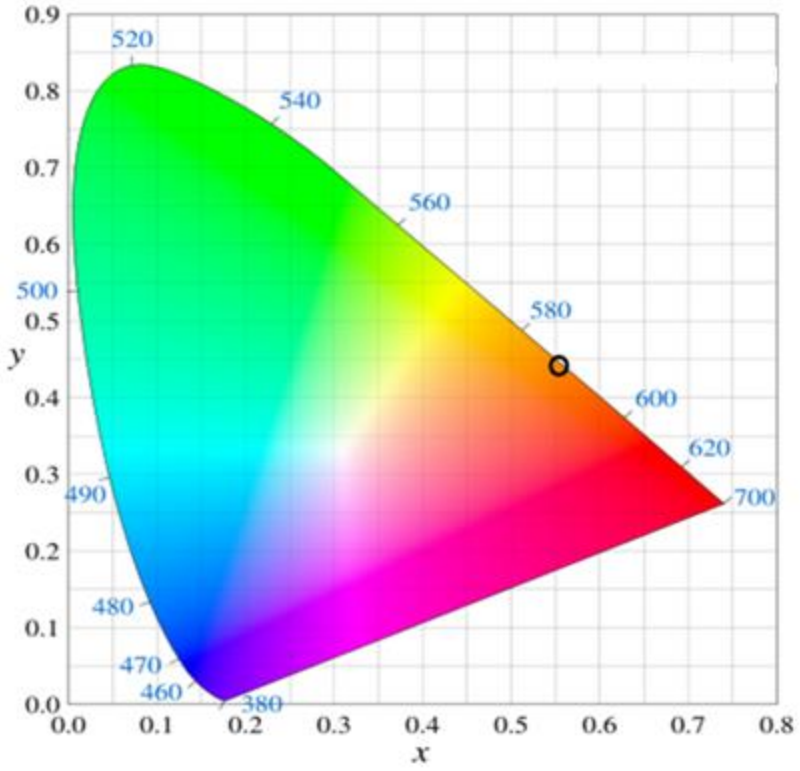

Figure 4.4 : CIE chromaticity diagram

The color coordinates for PVDT5050Sm5 are found to be 0.556 and 0.443, respectively and this result corresponds to hue of orange of CIE-1931 chromaticity diagram [38] as indicated in Figure 4.4 This dominant wavelength is determined by drawing a straight line from pure white light coordinates, i.e., equal energy point (0.33, 0.33) to the color coordinates of Sm^{3+} ions emission in the matrix. The purity of the color is found to be maximum (100%)

Reference

[1] I. Gorelikov and E. Kumacheva, Chem. Mater. **16** (2004) 4122.

[2] W. Caseri, Macromol. Rapid Commun. **21** (2000) 705.

[3] P. Judeinstein and C. Sanchez, J. Mater. Chem. **6** (1996) 511.

[4] S. Komarneni, J. Mater. Chem. **2** (1992) 1219.

[5] D.Y. Godovski, Adv. Polym. Sci. **119** (1995) 79.

[6] L.L. Beecroft and C.K. Ober, Chem. Mater. **9** (1997) 1302.

[7] A. Convertino, A. Capobianchi, A. Valentini and E.N.M. Cirillo, Adv. Mater. **15** (2003) 1103.

[8] A. Ershad-Langroudi , C. Mai, G. Vigier and R. Vassoile, J. Appl. Polym. Sci. **65**, (1997) 2387.

[9] G. Cartenuto, Y.S. Her and E. Matijevic, Ind. Eng. Chem. Res. **35** (1996) 2929.

[10] B. Wang, G. L. Wilkes, J. C. Hedrick, S. C. Liptak and J. E. McGrath, Macromolecules, **24** (1991) 3449.

[11] H. Lu , H. Wang and S. Feng, J. Photochem. Photobiol. A, **210** (2010) 48.

[12] M. Yoshida and P. N. Prasad, Chem. Mater. **8** (1996) 235.

[13] H. Jiang and A. K. Kakkar, Adv. Mater. **10** (1998) 1093.

[14] L. L. Hench and J.K. West, Chem. Rev. **90** (1990) 33.

[15] B. M. Novak, Adv. Mater. **5** (1993) 422.

[16] S.F. Wang, Y.R. Wang, K.C. Cheng and S.H. Chen, J. Mater. Sci. Mater. Electron. **21** (2010)104.

[17] K. Iuchi , Y. Ohko, T. Tatsuma and A. Fujishima, Chem. Mater. **16** (2004)1165.

[18] M. Biancardo, R. Argazzi and C.A. Bignozzi, Inorg. Chem. **44** (2005) 9619.

[19] A.F. Wells, Structural Inorganic Chemistry. Clarendon Press, Oxford, (1975).

[20] T. Peng, D. Zhao, H. Song, C. Yan, J Mol Catal A Chem, **238** (2005) 119.

[21] Q.Z. Yan, X. T. Su, Z.Y. Huang and C.C. Gea, J. Eur. Ceram. Soc. **26** (2006) 915.

[22] J. Zhu, J. Yang, Z.F. Bian, J. Ren, Y.M. Liu, Y. Cao, H.X. Li, H.Y. He and K.N. Fan, Appl. Catal. B, **76** (2007) 82.

[23] M. Zheng, M. Gu, Y. Jin, H. Wang, P. Zu, P. Tao and J. He, Mater. Sci. Eng. B, **87** (2001)197.

[24] W. T. Carnall, P. R. Fields, K. Rajnak, J. Chem. Phys. 49 (1968) 4424-4442.
[25] S. P. Sinha, Complexes of the rare earths, first ed., Pergamon Press, Oxford, 1966.
[26] B.R. Judd, Phys. Rev. 127 (1962) 750-761.
[27] G.S. Ofelt, J. Chem. Phys. 37 (1962) 511-520.
[28] Matras-Postolek M, Bogdal D (2010) Adv Polym Sci 230:221
[29] Hietala S, Holmberg S, Karjalainen M, Paronen M, Serimaa R, Sundholm F, Vahvaselka ¨ S (1997) J Mater Chem 7:721
[30] He F, Fan J, Lau S (2008) Polym Test 27:964
[31] Mawson S, Johnston KP, Combes JR, DeSimone JM (1995) Macromolecules 28:3182
[32] Scheinbeim JI (1999) In: Mark JE (ed) Poly(vinylidene fluoride). Oxford University Press Inc, New York
[33] Gregorio R Jr, Cestari M (1994) J Polym Sci B 32:859
[34] Tazaki M, Wada R, Okabe M, Homma T (1997) J Appl Polym Sci 65:1517
[35] Cheng LP (1999) Macromolecules 32:6668
[36] Salimi A, Yousefi AA (2004) J Polym Sci B 42:3487
[37] Hsu CC, Geil PH (1989) J Mater Sci 24:1219. doi:10.1007/ BF02397050
[38] E. Fred Schubert, Light Emitting Diodes, 2nd edition, Cambridge University Press, 2006.

CHAPTER 5

Summary

Abstract

This chapter deals with the summary of the project work

Polymer nanocomposites combine peculiar characteristics of polymers, such as structural flexibility, convenient processability and high thermal and mechanical stability with specific size dependent properties of inorganic nanocrystalline oxides, thus providing unique functions. Sol-gel synthesis of organic-inorganic hybrid materials for planar waveguides and devices has received growing interest due to its low cost processing and good suitability for doping and this synthesis technique also enables control of the organic–inorganic interaction at various molecular, nanometer and micrometer scales. Titania/polymer nanocomposites represent a new class of potential materials for optoelectronic applications. Titanium dioxide (TiO_2) is a very promising material for applications in many aspects such as solar energy conversion, photocatalysis, sensors and photochromic devices. PVDF with good film forming properties and mechanical properties may become additive of optical film to improve the film stress and compatibility with the substrate.

A new organic/inorganic hybrid material, PVDF/TiO_2 doped with Dysposium and Samarium was synthesised using non-aqueous sol gel process. The sample was also made into a thin film using dip coating technique. The powdered samples were optically characterised using UV-Vis NIR absorption technique and Photoluminescence technique. Bandgap obtained from the UV-Vs spectrum of the Dysposium doped sample was found to be comparatively high which finds wide applications in optical fields. The emission and excitation spectra of the Dysposium doped sample were studied.

Sammarium was doped in PVDF/TiO_2 matrix with varying concentrations of the matrix, out of which PT5050Sm5 sample was characterised optically. The absorption studies showed 18 peaks in the UV Vis NIR regions. The variation of α^2 versus photon energy for PT5050Sm5 hybrid material was studied. It is noted that the optical energy band gap (E_g) for

PT5050Sm5 hybrid material is 4.59 eV which shows that it is high bandgap material. From the absorption spectra nephleuxetic ratio and bonding parameter was calculated. The positive value of the bonding parameter showed that the Samarium ligand bonding in the matrix is of covalent nature. This was confirmed from the Judd Ofelt analysis. The experimental and oscillator strengths of the absorption transition from the ground state of Samarium $^{6}H_{15/2}$ to different excited states were calculated. The quantity of the fit has been expressed by the root mean square (r.m.s.) deviation of oscillator strengths. The small value of the rms deviation, 0.056×10^{-6} , showed the quality of the fit. Also the spectroscopic quality factor for the sample was found as 0.9349. The excitation spectrum matched well with the absorption spectrum of the sample. The emission spectrum of the sample was also studied.